Bulletin of Mathematical Biology, Vol. 59, No. 6, pp. 1077–1100, 1997
Elsevier Science Inc.

0092-8240/97 $17.00 + 0.00

S0092-8240(97)00063-3

ROLE OF FIBROBLAST MIGRATION IN COLLAGEN FIBER FORMATION DURING FETAL AND ADULT DERMAL WOUND HEALING

■ PAUL D. DALE,* JONATHAN A. SHERRATT† and PHILIP K. MAINI*
*Centre for Mathematical Biology,
Mathematical Institute,
24-29 St Giles',
Oxford OX1 3LB, U.K.

(*E.mail*: *pddale@maths.ox.ac.uk*, *maini@maths.ox.ac.uk*)

†Nonlinear Systems Laboratory,
Mathematics Institute,
University of Warwick,
Coventry CV4 7AL, U.K.

(*E.mail*: *jas@maths.warwick.ac.uk*)

Adult dermal wounds, in contrast to fetal wounds, heal with the formation of scar tissue. A crucial factor in determining the degree of scarring is the ratio of types I and III collagen, which regulates the diameter of the combined fibers. We developed a reaction-diffusion model which focuses on the control of collagen synthesis by different isoforms of the polypeptide transforming growth factor-β (TGFβ). We used the model to investigate the current controversy as to whether the fibroblasts migrate into the wound from the surrounding unwounded dermis or from the underlying subcutaneous tissue. Numerical simulations of a spatially independent, temporal model led to a value of the collagen ratio consistent with that of healthy tissue for the fetus, but corresponding to scarring in the adult. We investigated the effect of topical application of TGFβ and show that addition of isoform 3 reduces scar tissue formation, in agreement with the experiment. However, numerical solutions of the reaction-diffusion system do not exhibit this sensitivity to growth factor application. Mathematically, this corresponds to the observation that behind healing wavefront solutions, a particular healed state is always selected independent of transients, even though there is a continuum of possible positive steady states. We explain this phenomenon using a caricature system of equations, which reflects the key qualitative features of the full model but has a much simpler mathematical form. Biologically, our results suggest that the migration into a wound of fibroblasts and TGFβ from the surrounding dermis alone cannot account for the essential features of the healing process, and that fibroblasts entering from the underlying subcutaneous tissue are crucial to the healing process.

1. Introduction. Over the past 15 years, experiments on fetal wound healing have shown that little or no scar tissue is formed during the healing process. This is in direct contrast to adult repair, whose end product is a

scar that is weaker than normal skin and may cause functional impairment. The switch between these mechanisms is not sudden, but rather, there is a gradual transition from scarless healing to scar formation during the late fetal stages and early childhood (Adzick and Longaker, 1992; Armstrong and Ferguson, 1995).

Dermal tissue is very complex, consisting of many cell and matrix types. Recent experimental research has implicated the structural protein collagen as a key element of the healing process. There are two main types of collagen in the dermis, I and III, with type III collagen decorating the surface of the type I collagen fibril, so that a higher ratio of type III to type I results in thinner fibers (Whitby and Ferguson, 1991, 1992). In normal dermal tissue, the collagen fibers in the dermis exhibit a basket-weave–like arrangement, whereas in adult scar tissue, the fibers are longer and thinner than in normal skin, owing to higher levels of type III collagen (Mast *et al.*, 1992), and the fibers are oriented in the directions of greatest tension (Peacock, 1984).

In response to injury, fibroblasts migrate into the wound domain from the surrounding unwounded dermis and from the underlying subcutaneous tissue. The motile fibroblasts synthesize chains of amino acids called procollagens (McDonald, 1988), the process being activated by growth factors, including in particular transforming growth factor-β (TGFβ) (Appling *et al.*, 1989). The procollagens are activated by specific enzymes to form the combined collagen I and III fibers, whose diameter and orientation are crucial in explaining the difference between adult and fetal healing.

Much experimental work has been carried out on the effects of the addition of various growth factors on wounds, mainly adult wounds (Martin *et al.*, 1992; Pierce *et al.*, 1991). This work suggests that although the presence of other factors such as platelet-derived growth factors, fibroblast growth factor, hyaluronic acid, and other proteoglycans, does indeed regulate the healing process, their effects are negligible in comparison with TGFβ. We therefore chose to focus on TGFβ in this article. Dermal adult rat wounds injected at the margin with neutralizing antibody to TGFβs 1 and 2 have been shown to heal with reduced or no scarring, and with identical tensile strength and more normal dermal architecture than untreated wounds (Shah *et al.*, 1994). The advantageous effects of neutralizing antibody treatment wounds are not accompanied by a delay in healing (Shah *et al.*, 1992). Similar scar reduction results from exogenous addition of TGFβ3 (the peptide, not its antibody) to adult rat wounds (Shah *et al.*, 1995). Moreover, when either TGFβ1 or 3 is added exogenously to fetal wounds in rabbits (Krummel *et al.*, 1988), the final ratio of the collagens changes. In particular, it has been shown that topical application of TGFβ1 increases the amount of collagen III relative to collagen I (Murphy *et al.*,

1994). There is also recent evidence that anti-TGFβ strategies may reduce scarring in adult human wounds (Lin *et al.*, 1995).

In this article, in Section 2, we consider a mathematical model which investigates the effect of topical application of TGFβ on the collagen I : III ratio [the biological basis of the model is fully presented in Dale *et al.* (1996)]. In Section 3, we solve the model numerically for the fetal case in the absence of spatial variation, and then adapt the parameters for the adult healing process. By modeling the addition of growth factor, we investigate the implications for chemical reduction of adult scarring. In Section 4, we introduce diffusion terms to model an influx of fibroblasts from the wound edge. We show that healing waves moving in from the wound margins leave behind characteristic levels of types I and III collagen, independent of transient applications of TGFβ. This is in marked contrast to the spatially uniform model, in which such transient changes have a permanent effect on the collagen levels. We investigate this mathematically using a caricature model in Section 5 and discuss its biological implications in Section 6.

2. Mathematical Modeling. The process of wound healing is extremely complex, involving many different cell types and chemical regulators. The philosophy of our modeling approach is to focus on particular aspects of the wound-healing process and explore their implications in isolation; this is a philosophy broadly similar to that of *in vitro* experimentation. Specifically, we focus on the formation of collagen fibers, and in particular, on the ratio of type I to type III collagen, which controls fiber thickness. This ratio is used as a measure of the extent of scarring in some experimental studies [e.g., Knight *et al.* (1993)]. We consider the behavior of healing wavefront solutions in a model whose kinetic terms have been described previously (Dale *et al.*, 1996), and we begin by introducing these kinetics briefly.

Accumulation of collagen in the wound is dependent on the amount of collagen synthesized compared to that degraded by local enzymes. The control of collagen synthesis, secretion, crosslinking, and degradation is incompletely understood, but collagen is certainly critical for the return of tissue integrity and strength (Jeffrey, 1992; Krieg, 1995). During the healing process, motile fibroblasts of density $f(\underline{r}, t)$ at position $\underline{r}$ and time t synthesize much of the intercellular material, including TGFβ and other polypeptide growth factors, and different collagens and collagenases. TGFβ is autoinductive (Lin *et al.*, 1995), and experiments indicate that the growth factor stimulates the secretion of collagen by fibroblasts (Murphy *et al.*, 1994). Collagenase is responsible for the downregulation of collagen. The collagen level in a healed wound is thus dynamically dependent on fibroblasts, TGFβ, and collagenases, as illustrated schematically in Fig. 1. To

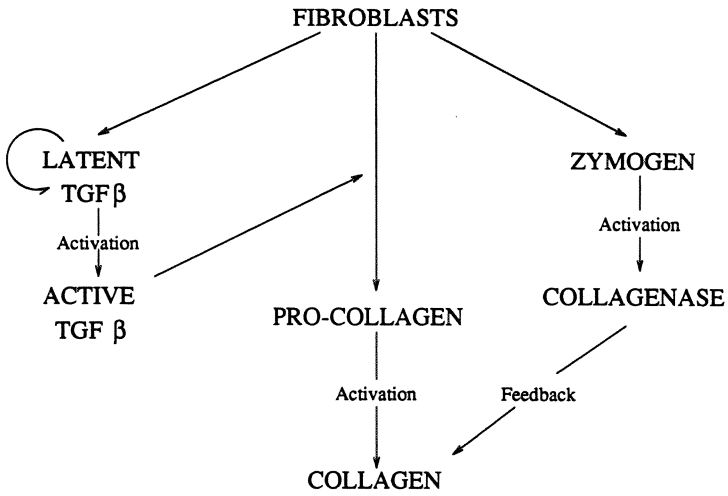

Figure 1. Schematic representation of the interactions between growth factors, proteins, fibroblasts, and enzymes during the wound-healing process. The fibroblast cells secrete precursors to both collagen and collagenase, so that there is a feedback control loop. They also secrete growth factors which regulate collagen production, again in a precursor (latent) form. The various precursor forms are made active via enzymes which are released as part of the response to wounding, and are absent in unwounded skin. It is this feature of the system that results in a continuous range of possible healed states. Our full-model equations contain variables reflecting the presence of two isoforms of TGFβ, two types of collagen, and, correspondingly, two types of zymogen.

capture the essential features of the healing process, we extend this basic framework to explicitly include different types of growth factors, collagens, and collagenases. We must emphasize that many other factors contribute to collagen assembly: for example, glycosaminoglycans and proteoglycans (Flint *et al.*, 1984); we neglect such factors to focus in detail on the particular control loop shown in Fig. 1.

Fibroblast proliferation and collagen synthesis are upregulated by TGFβs, and recent research has shown that the ratio of different TGFβ isoforms is a key factor (Chen *et al.*, 1993). In our model, we represent active TGFβ via the variables $\beta_1(\underline{r}, t)$ (representing isoforms 1 and 2) and $\beta_3(\underline{r}, t)$ (representing isoform 3). The model focuses on collagens I and III, denoted by $c_1(\underline{r}, t)$ and $c_3(\underline{r}, t)$, respectively. These are the major proteins involved in dermal architecture, although there is some recent evidence that other collagen types, which we neglect, may be expressed during wound healing and influence scar quality. We also introduce two different collagenases, types I and III, represented by $s_1(\underline{r}, t)$ and $s_3(\underline{r}, t)$, respectively, which are responsible for the breakdown of collagen fibers.

As they enter the wound, fibroblasts are stimulated via autocrine regulation (Roberts and Sporn, 1990) to secrete growth factors, collagen, and

collagenases in latent forms (McDonald, 1988). The two major isoforms of latent TGFβ are represented by $l_1(\underline{r},t)$ and $l_3(\underline{r},t)$, respectively, and we focus on two types of procollagens, types I and III, denoted by $p_1(\underline{r},t)$ and $p_3(\underline{r},t)$, and the corresponding latent collagenases, known as zymogens I and III ($z_1(\underline{r},t)$ and $z_3(\underline{r},t)$, respectively). During the inflammation stage of wound healing, white blood cells release a range of enzymes which activate these growth factors, procollagens, and zymogens (Sinclair and Ryan, 1994); the pools of enzyme are rapidly degraded during the healing process. Since detailed descriptions of the various enzymes are not currently available, we represent their effects by generic enzymes $e_1(\underline{r},t), e_2(\underline{r},t), e_3(\underline{r},t)$, and use the law of mass action to model the activation of latent TGFβ1 and 3 and type I and type III procollagen and zymogens.

To reflect these various points, we use the following model equations:

Rate of increase of fibroblast density	=	Fibroblast migration	+	Mitotic generation	−	Natural loss
Rate of increase of latent TGFβ concentration	=	Chemical diffusion	+	Production by fibroblasts	−	Natural decay
					−	Activation by enzyme
Rate of increase of active TGFβ concentration	=	Chemical diffusion	+	Activation of latent form by enzyme	−	Natural decay
Rate of increase of enzyme 1	=	− Activation of latent TGFβ				
Rate of increase of enzyme 2	=	− Activation of procollagens				
Rate of increase of enzyme 3	=	− Activation of zymogens				
Rate of increase of procollagen	=	Secretion by fibroblasts	−	Natural decay	−	Conversion by enzyme
Rate of increase of collagen	=	Activation of procollagen by enzyme	−	Degradation by collagenases		
Rate of increase of zymogens	=	Secretion by fibroblasts	−	Natural decay	−	Activation by enzyme
Rate of increase of collagenase	=	Activation of zymogens by enzyme	−	Natural degradation		

With the two isoforms of TGFβ and the two collagens and collagenases that we are considering, the corresponding mathematical equations have the form

$$\frac{\partial f}{\partial t} = D_1\nabla^2 f + (A_1 + A_2\beta_1 + A_3\beta_3) f\left(1 - \frac{f}{k_1}\right) - A_4 f \tag{1a}$$

$$\frac{\partial l_1}{\partial t} = D_2\nabla^2 l_1 + \frac{A_5 f l_1}{1 + A_6 l_3 + A_7 l_1} - A_8 l_1 - A_{16} e_1 l_1 \tag{1b}$$

$$\frac{\partial l_3}{\partial t} = D_3\nabla^2 l_3 + \frac{A_9 f l_3}{1 + A_{10} l_3} - A_{11} l_3 - A_{17} e_1 l_3 \tag{1c}$$

$$\frac{\partial \beta_1}{\partial t} = D_4\nabla^2 \beta_1 + A_{12} e_1 l_1 - A_{13}\beta_1 \tag{1d}$$

$$\frac{\partial \beta_3}{\partial t} = D_5\nabla^2 \beta_3 + A_{14} e_1 l_3 - A_{15}\beta_3 \tag{1e}$$

$$\frac{de_1}{dt} = -e_1(A_{16} l_1 + A_{17} l_3) \tag{1f}$$

$$\frac{de_2}{dt} = -e_2(A_{18} p_1 + A_{19} p_3) \tag{1g}$$

$$\frac{de_3}{dt} = -e_3(A_{40} z_1 + A_{41} z_3) \tag{1h}$$

$$\frac{dp_1}{dt} = (A_{20} + A_{21}\beta_1 + A_{22}\beta_3) f - A_{23} p_1 - A_{18} e_2 p_1 \tag{1i}$$

$$\frac{dp_3}{dt} = (A_{24} + A_{25}\beta_1 + A_{26}\beta_3) f - A_{27} p_3 - A_{19} e_2 p_3 \tag{1j}$$

$$\frac{dc_1}{dt} = A_{28} p_1 e_2 - A_{29} s_1 c_1 \tag{1k}$$

$$\frac{dc_3}{dt} = A_{30} p_3 e_2 - A_{31} s_3 c_3 \tag{1l}$$

$$\frac{dz_1}{dt} = \frac{A_{32}}{1 + A_{33}\beta_1 + A_{34}\beta_3} f c_1 - A_{35} z_1 - A_{40} e_3 z_1 \tag{1m}$$

$$\frac{dz_3}{dt} = \frac{A_{36}}{1 + A_{37}\beta_1 + A_{38}\beta_3} f c_3 - A_{39} z_3 - A_{41} e_3 z_3 \tag{1n}$$

$$\frac{ds_1}{dt} = A_{42} z_1 e_3 - A_{43} s_1 \tag{1o}$$

$$\frac{ds_3}{dt} = A_{44} z_3 e_3 - A_{45} s_3. \tag{1p}$$

Thus, following many previous authors (Murray *et al.*, 1988; Sherratt and Murray, 1990; Chaplain *et al.*, 1995), we represent random cell movement via linear diffusion. Note that active TGFβ has a complex regulatory role during wound healing, upregulating fibroblast proliferation (Krummel *et al.*, 1988) and procollagen synthesis (Appling *et al.*, 1989), but inhibiting the secretion by fibroblasts of the zymogens (Jeffrey, 1992).

In Equation (1), the A_i's are constant parameters. The estimation of dimensional parameter values is essential for biologically realistic model predictions, and our equations contain a large number of parameters in comparison to the limited source of experimental data, which enables us to estimate only a few with good accuracy. Data are available for the normal dermal levels of fibroblasts (Morgan and Pledger, 1992), growth factors (Streuli *et al.*, 1993), and collagen I and III (Merkel *et al.*, 1988), together with fibroblast migration rates (Bard and Hay, 1975). We know the molecular weights of active and latent TGFβ, so that we can use the Stokes–Einstein formula to derive an estimate for the diffusion coefficients. We also have good data for cell-cycle times and the half-life of growth factors. Since we know the time scale of the healing process, we can obtain order of magnitude estimates for some of the remaining parameters by fitting model solutions with experimental data from fetal wound-healing studies. However, there are still a number of parameters for which we cannot get good estimates. To address this, we have performed parameter sensitivity analysis, by perturbing each parameter in turn and determining the effect on the model solution. The analysis (not shown) indicates that none of the unknown parameters are crucial in explaining the difference between adult and fetal healing. In the remainder of the article, we use the parameter values given in the legend to Fig. 2, with appropriate changes for adult rather than fetal repair [see Dale *et al.* (1996) for full details].

There has been little experimental work on the role of diffusion of growth factors and migration of fibroblasts into the wound milieu. In this absence of experimental detail, there is a controversy concerning whether fibroblasts migrate into the wound from the underlying subcutaneous tissue or from the neighboring dermis. In the latter case, a spatially dependent model is essential to reflect variations in the plane of the skin. However, in the former case, spatial variations within the wound will be quite small, since the wound depth is much smaller than a typical wound dimension; therefore, we can reasonably consider a purely temporal model, given by setting $D_1 = D_2 = D_3 = D_4 = D_5 = 0$.

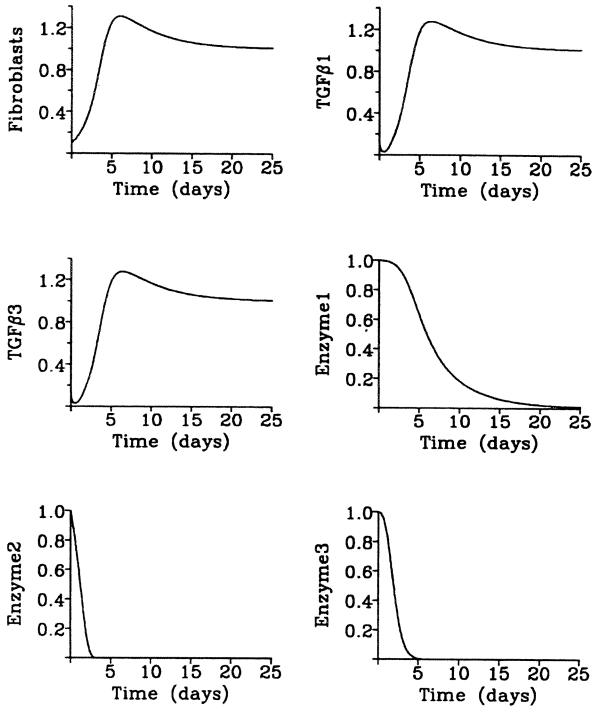

Figure 2. Numerical solution of the model equations for the 25 days postwounding, for parameter values corresponding to fetal skin. We impose the initial conditions corresponding to small levels of fibroblasts and latent growth factors, and high initial concentrations of our three generic enzymes, which are produced as a response to wounding. We assume that the collagens and collagenases are initially absent in the wound. The fibroblasts and chemical regulators rapidly attain their steady-state values and the collagen I and III densities evolve so that their final healed ratio is approximately 3:1, as in normal fetal skin. Specifically, we take as initial conditions $f(0) = l_1(0) = l_3(0) = 0.1$, $e_i(0) = 1$, $i = 1, 2, 3$, $c_1(0) = c_3(0) = s_1(0) = s_3(0) = 0$. We express f, l_1, l_3 as a proportion of the corresponding unwounded levels, which we denote by f^0, l_1^0, and l_3^0; we estimate these parameters as $f^0 = 10^5$ ml^{-1} (Morgan and Pledger, 1992), and $l_1^0 = l_3^0 = 2$ ng ml^{-1} (Streuli *et al.*, 1993). The collagen densities c_1 and c_3 are expressed as a proportion of the unwounded level of collagen I in normal fetal dermis, which is approximately $c_1^0 = 12.5$ μg mg^{-1} dry weight (Merkel *et al.*, 1988). The enzyme concentrations e_i are expressed as a proportion of the initial levels, e_i^0, say, and collagenase levels are expressed as a proportion of the maximum levels observed on wounding, denoted s_1^0. A detailed derivation of the dimensionless parameter ratios is found in Dale *et al.* (1996).

3. Temporal Model. In this model, the underlying tissue is considered to be the sole source of fibroblasts. The temporal model equations have two types of steady state: the wounded state, with every variable zero; and healed steady states, with all the variables at their normal dermal level except for collagen I and III, which can take any value. This continuum of steady states is a crucial property of the model, since experimental results

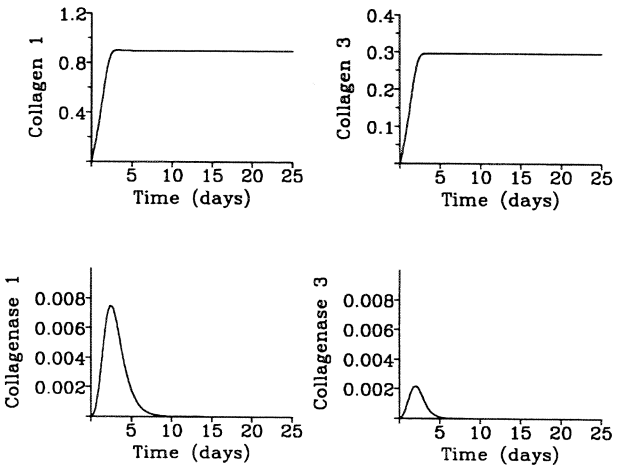

Figure 2. (*Continued*).

indicate that the final healed levels of collagen I and III can be permanently altered by transient exogenous application of TGFβs. Linear stability analysis confirms that in the model equation (1), for the parameter values we are using, the zero steady state is unstable, whereas the healed equilibrium is always stable, as required for biological realism.

To numerically simulate wound healing, we use initial conditions in which all the variables are at their wounded equilibrium levels, except for small perturbations applied to the fibroblast and growth factor levels. Numerical solutions for parameters corresponding to fetal skin indicate a rapid initial increase of fibroblasts and TGFβ before they settle down to the normal dermal levels, in agreement with experimental observations (Ferguson and Howarth, 1992). The enzyme concentrations decrease to zero with time, and after an initial increase, the collagenase concentrations decay to zero. The new levels of collagen I and III are quickly attained and are maintained throughout the healing process in a ratio of about 3:1 (Fig. 2). Thus, both the density and ratio of collagen I:III after healing agree with the experimental data. Further numerical simulations indicate that addition of TGFβ1 increases this ratio, implying that the collagen fibrils in the healed wound are thinner in diameter than in normal fetal wounds, which is a characteristic of scarring. In contrast, when isoform 3 is added, the ratio of collagen I to III increases, corresponding to thicker fibers, which could reflect either high-quality repair or possible healing abnormalities (Zhang *et al.*, 1995; Olsen *et al.*, 1996). Moreover, the simulations suggest a saturating concentration of 0.4 μg ml^{-1} for TGFβ, in broad agreement with experiments (Krummel *et al.*, 1988), and that addition very soon after wounding is essential (Dale *et al.*, 1996), also consistent with experiments (Shah *et al.*, 1994).

A key aspect of wound-healing studies is to explain the difference between fetal and adult healing. We have thus far used known results for fetal healing to fix a number of parameters: in particular, the return of collagen levels to those in unwounded skin in simulations of fetal healing is determined by our choice of parameters. We now adapt our model to study adult healing by changing a small number of parameters to reflect the known key differences between fetal and adult skin. The main differences are that the cell-cycle time for adult fibroblasts is much slower than in the fetal case, and that the unwounded concentrations of TGFβ1 and 3 in adult dermal tissue are 80 and 40 ng ml^{-1}, respectively (Roberts and Sporn, 1990), a 20-fold increase on the corresponding fetal levels. The total collagen content in normal adult dermal tissue is also about 20-fold higher, at 331 μg/mg dry weight (Merkel *et al.*, 1988), 15% of which is type III.

Numerical solutions for these new parameters show fibroblasts and growth factors settling down to the healed levels after a much longer period of time (the realistic repair time of about 60 days), whereas the collagens rapidly attain new healed levels, with higher collagen content in a ratio of 3.6:1, in fair agreement with the experimentally determined ratio of 4:1, and corresponding to thinner collagen fibers than in normal skin, where the ratio is about 5.6:1. This prediction of scarring in adult skin is a firm prediction of the model, based on known parameter changes from the fetal parameter set, and not a consequence of parameter finetuning.

Addition of TGFβ1 again results in an increased level of collagen III, implying thinner fibers, whereas when TGFβ3 is added, we observe collagen levels corresponding to 15% type III collagen, in agreement with normal dermal tissue (Dale *et al.*, 1996). Hence, by solving our temporal model for healing, which follows the evolution in time of fibroblast density and TGFβ, collagen, and collagenase concentrations, we predict that scar tissue formation is reduced by the early addition of TGFβ3.

4. Reaction-Diffusion Model. In Section 3, we studied the model [Eq. (1)] in the absence of spatial variation, corresponding to the main source of fibroblasts being the underlying subcutaneous tissue. We now consider the system of reaction diffusion equations, which assumes that the cells and growth factors enter the wound space predominantly from the surrounding unwounded dermis. As we are considering full-thickness, excisional, clean wounds, we assume that no fibroblasts, growth factors, collagen, or collagenase are initially present within the wound domain. We also assume that all the model variables are initially at their unwounded levels outside the wound milieu, so that the initial conditions have a step function form. The initial, inflammatory response to wounding causes a pool of activating enzymes to be released within the wound; this enters our model as an initial condition for the variables e_1, e_2, e_3, and is the only source of these

enzymes. To facilitate simulation, we consider a one-dimensional spatial domain, with the spatial coordinate x in the plane of the skin, corresponding to a linear slash wound. Since our basic interest is in wave solutions corresponding to healing, the most convenient domain is $-L < x < x_\infty$, where $x > 0$ is the initial wound region, and $x < 0$ represents surrounding unwounded dermis. We rescale x so that $L = 1$, and we take x_∞ as sufficiently large to enable healing fronts to develop. The appropriate boundary conditions are thus symmetric conditions at $x = x_\infty$, with all variables fixed at their unwounded levels at $x = -1$.

Numerical solutions of the model equations for the parameters corresponding to fetal skin over a large spatial domain show waves of cells and growth factors moving into the wound with constant speed and shape, with the steady states behind the waves corresponding to the unwounded nondimensional level (Fig. 3). The solution profiles for collagen I and III also show fronts moving into the wound domain, evolving to new steady-state levels for both collagen I and III, with a ratio of 3:1, in agreement with the unwounded dermal tissue. The collagenase equations show wave pulses moving into the wound, and both collagenase I and III decay to the zero dermal level. The dimensional wave speed is about 0.5 μm h^{-1}, indicating a healing time of about 8 days for a 0.1-mm wound; the experimentally observed time is 5 days (Shah *et al.*, 1992). Solutions for the adult case again exhibit traveling waves, but in this case the ratio of collagen I to III is about 3.6:1, which corresponds to thinner, more densely packed collagen fibers than in unwounded skin (ratio about 5.6:1), and thus scar tissue formation; also the healing rate is almost an order of magnitude slower.

In Section 3, we described the way in which simulations of the spatially homogeneous equations exhibit the phenomenon of a spectrum of collagen I and III steady states; the values are dependent on the initial amounts of TGFβ, collagen I and III, and collagenase I and III present in the wound. We now look for the same behavior in the reaction-diffusion model by solving the full system with different initial conditions. We first alter the initial conditions to reflect the addition of large concentrations of (latent) TGFβ1 to the initially wounded region. Numerical simulations show fronts of fibroblasts and the different isoforms of growth factors moving into the wound with constant speed and shape. The profiles for collagen I and III show a sudden change at the initial wound edge, and the wave of collagens initially attains a steady-state value in agreement with the spatially homogeneous solution. However, the equilibrium values increase with time and settle at levels which are the same as those observed in the absence of exogenous growth factor application (Fig. 4). This result suggests that dependence of the final steady state on the transient application of TGFβs, which is observed in experiment and is captured by the temporal model, is lost when the model is extended to include spatial variation.

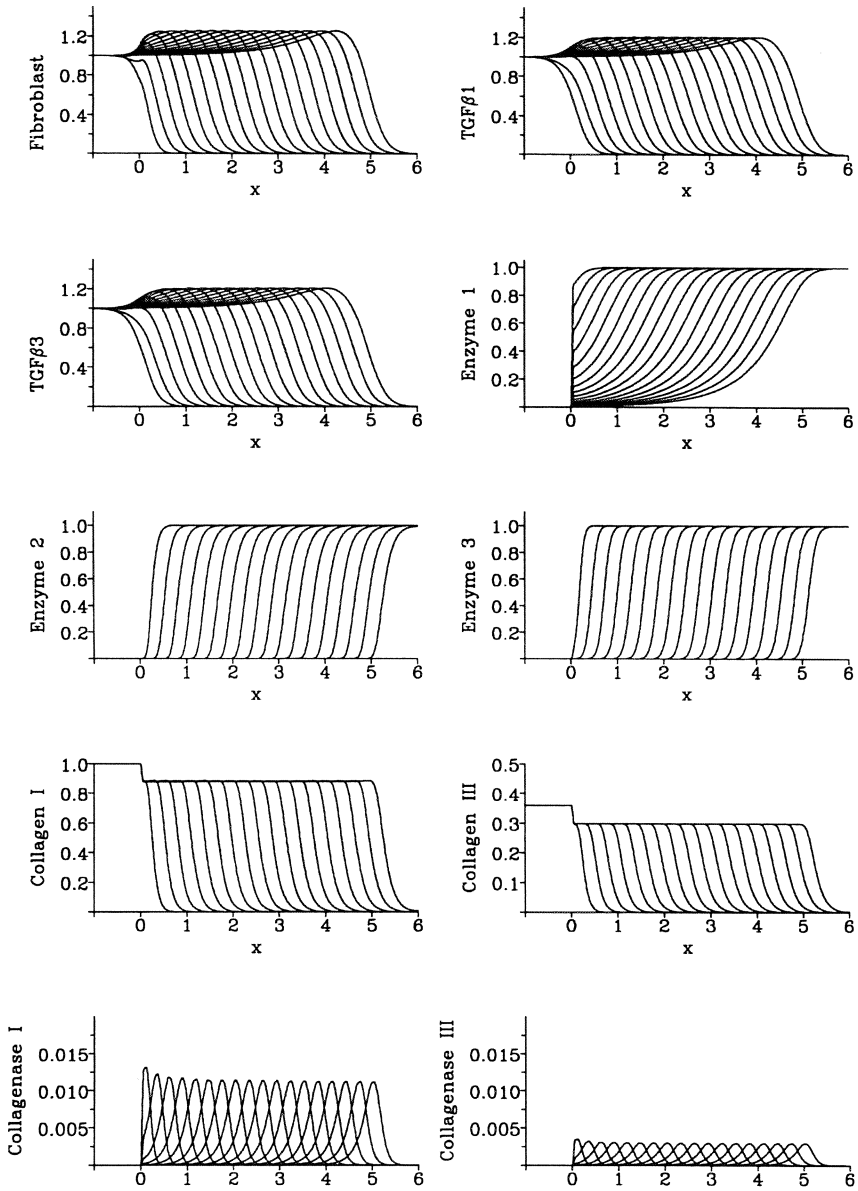

Figure 3. During the wound-healing process, waves of fibroblasts and TGFβ, together with fronts of collagen I and III, are observed to move into the wound domain. Here, we show numerical solutions of the model Equation (1) over an infinite domain, indicating the field variables as functions of space at equal time intervals of 36 h, using linear geometry. The parameters are as in Fig. 2, with the additional dimensionless parameter ratios: $D_1/L^2T = 0.015$, $D_2/L^2T = 0.25$, $D_3/L^2T = 0.25$.

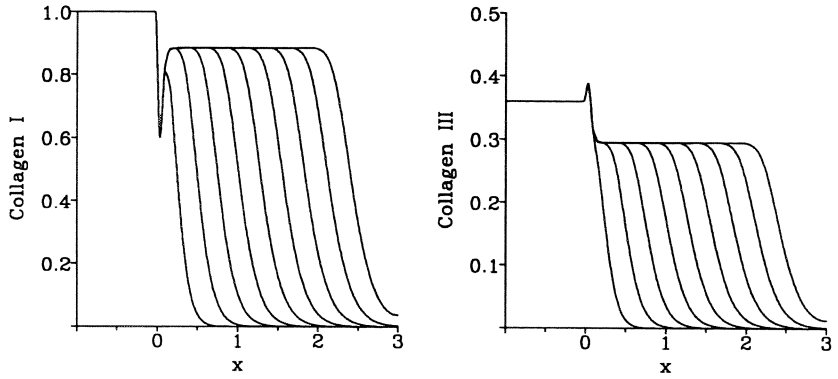

Figure 4. Experimental data indicate that the final levels of collagen I and III are altered by the exogenous application of different of TGFβ. Numerical solutions of the full system of partial differential Equation (1) are shown with smooth initial conditions and addition of TGFβ1, at equal time intervals of 36 h. The parameters are as in Fig. 3. The steady-state levels of collagen I and III undergo a transient change but eventually evolve to the same level attained in the absence of excess chemical.

To investigate this further, we try to force the collagens to attain different steady states by imposing initial conditions in which the level of collagen outside the wound domain is that predicted by the temporal model, rather than that corresponding to normal skin, in addition to exogenous application of TGFβ1. However, the profiles of collagen I and III again show only transient changes before evolving to untreated levels. Qualitatively similar results are obtained for the addition of TGFβ3. Of course, the healed steady-state levels do depend on the model parameter values, but extensive numerical simulations suggest that the insensitivity of the collagen levels to TGFβ addition holds for a wide range of parameter values.

The model system has a continuum of possible positive collagen steady states, but numerical solutions for the addition of TGFβ suggest that one particular steady state is selected behind the healing wave. In contrast, experiments show that addition of TGFβ does permanently alter the collagen density and fiber diameters. We have shown that whereas the assumption that the underlying tissue is the major source of fibroblasts leads to model results that agree with experimental observation, the alternative assumption that fibroblasts diffuse into the wound from surrounding tissue leads to model results that fail to capture this key experimental observation. Hence, our model suggests that migration of fibroblasts and TGFβ from the surrounding dermis alone cannot account for the essential features of the healing process.

5. Caricature Model. The reaction diffusion system [Eq. (1)] is too complicated for further analysis, and we thus attempt to study it via a caricature system. This is of a very much simpler form than Equation (1), but retains the key feature of wave propagation, with a trivial steady state ahead of the wave and a continuum of possible nontrivial states, one of which is selected behind the wave. Our objective in studying this caricature model is to understand this selection process.

We consider a system of equations for two variables, $u(x,t)$ and $v(x,t)$, which are functions of time t and position x in a semi-infinite, one-dimensional spatial domain. Intuitively, one can regard u as mimicking the fibroblast population in the full model, with v mimicking one of the types of collagen. However, there is no formal correspondence, and the purpose of the caricature model we discuss here is to gain mathematical insight into a system that is analogous to, but simpler than, the full model, in the hope that this insight can be extended to the full model. The simple system is the following

$$\frac{\partial u}{\partial t} = D\frac{\partial^2 u}{\partial x^2} + u(1-u) \tag{2a}$$

$$\frac{\partial v}{\partial t} = \alpha u(1-u) - (1-u)v \tag{2b}$$

where D and α are both positive constants. Thus, u satisfies the Fisher equation (Fisher, 1937), which decouples from the v equation (2b). The particular form of this caricature system is, of course, arbitrary. However, it has two basic features that are chosen deliberately to mimic aspects of the full system (1):

1. The decoupling of the u equation from the dynamics of v mimics the fact that in the full model, Equations (1a–f) decouple from (1g–p). That is, the dynamics of fibroblasts, active and latent growth factor, and enzyme 1 are unaffected by the collagen, collagenases, and remaining enzymes.
2. In addition to the trivial steady state $u = v = 0$, there is a continuum of steady states with $u = 1$ and v taking any value. This mimics the existence of a continuum of steady states for collagen I and III levels in the healed equilibrium solutions of the full model.

In the full model, we began by considering a temporal model, with cells undergoing proliferation and death but no migration. Analogous to this, we consider the pair of ordinary differential equations given by setting $D = 0$, with initial conditions $u = u_0$ and $v = 0$ at time $t = 0$, where u_0 is an

arbitrary constant. Solving this system gives

$$u(t) = \frac{1}{1+Ae^{-t}} \quad \text{and} \quad v(t) = \frac{\alpha A(A+2)}{2(A+1)^2}(1+Ae^{-t}) - \frac{(\alpha A^2 e^{-t} + 2\alpha A)}{2(A+e^{t})}$$

where the constant $A = -1 + 1/u_0$. This implies that as $t \to \infty$, $u \to 1$ and $v \to v^* \equiv \alpha(1-u_0^2)/2$. Remembering that u mimics cell density, we are primarily interested in cases in which $u_0 \ll 1$, so that $v^* \approx \alpha/2$.

We now solve the reaction-diffusion system ($D > 0$), with step function initial conditions and zero flux boundary conditions, as in the full model. Specifically, we use a spatial domain $-1 < x < x_\infty$, with $u(x,0) = v(x,0) = 1$ for $x < 0$ and 0 for $x > 0$, and with $\partial u/\partial x = \partial v/\partial x = 0$ at $x = x_\infty$ and $u = v = 1$ at $x = -1$. Here, x_∞ is suitably large, chosen to numerically simulate a semi-infinite domain. For u, which satisfies the standard Fisher equation, such initial conditions evolve to waves moving with constant shape and with speed $2\sqrt{D}$ (Kolmogoroff *et al.*, 1937). Our numerical simulations also show traveling fronts for the variable v, moving with the u wave (Fig. 5). Behind these fronts, v has a constant value v^* that is slightly greater than $\alpha/2$; there is also a sharp transition in v, at $x = 0$, from $v = 1$ to $v = v^*$.

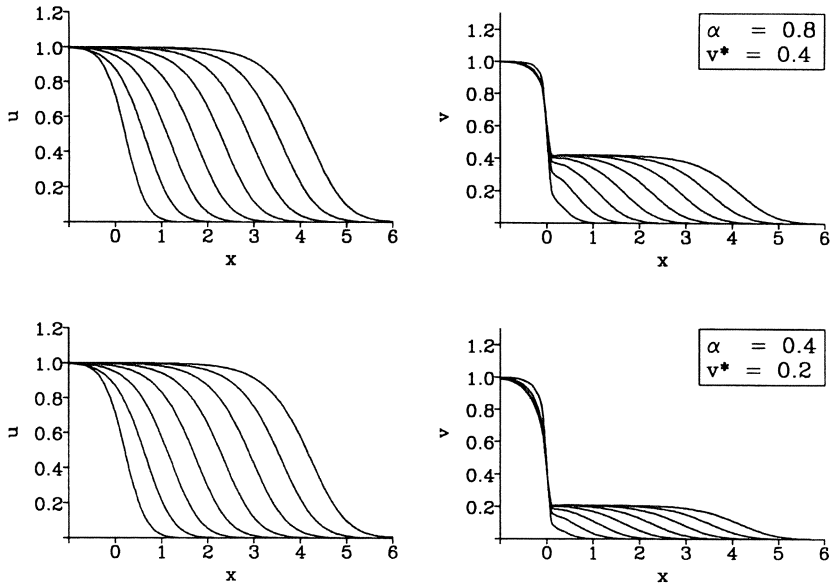

Figure 5. Numerical solutions of the nonlinear parabolic partial differential Equation (2) with step function initial conditions, showing the change in u and v with space, at equal time intervals. The diffusion coefficient D is taken to be 0.05, and we vary α as shown. The steady-state v^* is observed to be approximately $\alpha/2$.

Altering the values of $u(x,0)$ and $v(x,0)$ (i.e., the initial values) in $x<0$ has no effect on the observed value of v^*, suggesting that as in the full model (1), there is only one possible wavefront solution, even though any value of v is a steady state when $u=1$. A natural question to ask is whether this behavior is dependent on the wave speed. To answer this, we considered different initial conditions of the form $u(x,0)=v(x,0)=\min\{1,e^{-Rx}\}$. For u, it is a standard result that such initial conditions evolve to wavefronts moving with speed a, given by

$$a=\begin{cases} DR+1/R, & R\leqslant 1/\sqrt{D} \\ 2\sqrt{D}, & R\geqslant 1/\sqrt{D} \end{cases}$$

(Rothe, 1978), where a is the wave speed. Numerical solutions of Equation (2) indicate that v evolves to wavefronts moving with speed a also, and that the value $v=v^*$ behind these fronts has a continuous dependence on a, although with a very small variation (about 2% in total) (Fig. 6). Again, the value of v^* is independent of the initial value of v in $x<0$.

These simulations of the caricature model suggest that although there exists a continuum of nontrivial steady states $u=1$, v arbitrary, a particular value of v is always selected behind a wavefront of a given speed. This value is dependent on the wave speed, but only slightly, and its value is always approximately $\alpha/2$. To investigate this further, we consider the

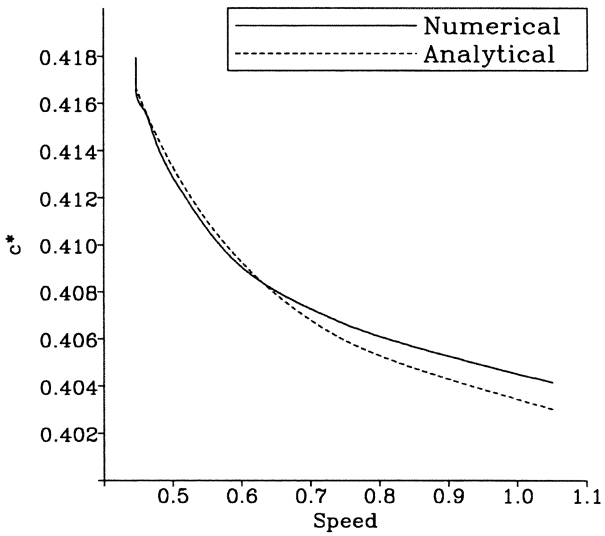

Figure 6. In the caricature model, the steady-state value v^* is independent of the initial values of u and v in $x<0$. To investigate the dependence on the wave speed, we impose exponentially decaying initial conditions. Here, we show the numerically and analytically determined change in the steady-state v^* as the wave speed a varies.

ordinary differential equations satisfied by traveling wave solutions of Equation (2). Setting $u(x,t) = U(z)$ and $v(x,t) = V(z)$, where $z = x - at$, U and V satisfy

$$DU'' + aU' + U(1-U) = 0 \tag{3a}$$

$$aV' + \alpha U(1-U) - (1-U)V = 0 \tag{3b}$$

where the prime denotes d/dz.

This third-order system has a trivial steady state $U = U' = V = 0$, and a line $\mathscr{L}$ of nontrivial equilibria $U = 1$, $U' = 0$, V arbitrary. In the three-dimensional phase space, a traveling front solution has the form of a heteroclinic connection from the line $\mathscr{L}$ to the trivial steady state. Straightforward linear analysis shows that at $(0,0,0)$, there is a two-dimensional stable manifold, while the eigenvalues are the same at each point on $\mathscr{L}$, with one positive, one negative, and one zero. The zero eigenvalue corresponds to neutral stability to perturbations along the line of steady states.

This linear analysis does not permit any conclusions about the number of traveling wave solutions, since one trajectory originates from each point on $\mathscr{L}$, and any or all of these trajectories could approach $(0,0,0)$ via the two-dimensional stable manifold. However, the decoupling of Equation (3a) and (3b) enables fuller conclusions to be drawn. It is a standard result that in Equation (3a), there is exactly one solution satisfying the end conditions $U(-\infty) = 1$, $U(+\infty) = 0$, for all wave speeds $a \geqslant 2\sqrt{D}$ (Kolmogoroff *et al.*, 1937). Substituting this solution into Equation (3b) gives a first-order initial value problem, so that the solution for V can be determined given only the condition $V(+\infty) = 0$. Thus, for each value of the wave speed a, the value $v^* = V(-\infty)$ behind the wavefront is uniquely determined via this solution for V.

Asymptotic solutions of the caricature model. We have shown that the value of v^* is uniquely determined for each value of the wave speed $a \geqslant 2\sqrt{D}$. In this section, we exploit our argument further by extending to our caricature equations (2), the regular perturbation method of Canosa (1973) for determining the traveling wave solutions of Fisher's equation. The basis of Canosa's approach is to use $\epsilon = D/a^2$ ($\leqslant 1/4$) as a perturbation parameter, and to stretch the traveling wave coordinate, via $\zeta = z/a$. Using these for Equation (3) gives

$$\epsilon D \frac{d^2U}{d\zeta^2} + \frac{dU}{d\zeta} + U(1-U) = 0 \tag{4a}$$

$$\frac{dV}{d\zeta} + \alpha U(1-U) - (1-U)V = 0. \tag{4b}$$

We look for solutions as a regular perturbation series in ϵ, of the form

$$U(\zeta;\epsilon) = U_0(\zeta) + \epsilon U_1(\zeta) + \epsilon^2 U_2(\zeta) + \cdots$$
$$V(\zeta;\epsilon) = V_0(\zeta) + \epsilon V_1(\zeta) + \epsilon^2 V_2(\zeta) + \cdots$$

with boundary conditions

$$U_0(-\infty) = 1, \qquad U_0(\infty) = 0, \qquad U_0(0) = 1/2, \qquad V_0(\infty) = 0$$

and

$$U_i(\pm\infty) = 0, \qquad U_i(0) = 0, \qquad V_i(\infty) = 0 \qquad \text{for} \quad i = 1,2,\ldots.$$

The conditions on U_i at $\zeta = 0$ are chosen simply to fix the origin of ζ.

Substituting these expansions into Equation (4) and equating powers of ϵ gives

$\mathscr{O}(1)$:
$$\frac{\partial U_0}{\partial \zeta} + U_0(1 - U_0) = 0$$
$$\frac{\partial V_0}{\partial \zeta} - (1 - U_0)V_0 = \alpha U_0(1 - U_0)$$

$\mathscr{O}(\epsilon)$:
$$\frac{\partial U_1}{\partial \zeta} + U_1(1 - 2U_0) = -D\frac{\partial^2 U_0}{\partial \zeta^2}$$
$$\frac{\partial V_1}{\partial \zeta} - V_1(1 - U_0) = \alpha U_1(1 - 2U_0) + U_1 V_0,$$

with further equations for higher-order terms. Since the U_i equations decouple from the V_i equations, we solve these first subject to the boundary conditions, giving

$$U_0(\zeta) = \frac{1}{1 + e^{\zeta}}$$
$$U_1(\zeta) = \frac{e^{\zeta} D}{(1 + e^{\zeta})^2} \log\left(\frac{4e^{\zeta}}{(1 + e^{\zeta})^2}\right).$$

Substituting these expressions into the equations for V_0 and V_1 gives

$$V_0(\zeta) = \frac{\alpha}{2(1+e^{\zeta})}$$

$$V_1(\zeta) = \frac{1}{12(1+e^{\zeta})^2}\left(\alpha D - 3\alpha D e^{\zeta} + 6\alpha e^{\zeta} D \log\left(\frac{4e^{\zeta}}{(1+e^{\zeta})^2}\right)\right)$$

In particular, note that to leading order, $V = \alpha U/2$.

From this solution, we can derive v^* as $V(-\infty)$, giving

$$v^* = \frac{\alpha}{2} + \frac{\epsilon\alpha D}{12} + O(\epsilon^2) \approx \frac{\alpha}{2} + \frac{\alpha D}{12a^2} \tag{6}$$

in terms of the original variables. This approximation compares extremely well with the numerical results described previously (Fig. 6). Note in particular that since a can take any value $\geqslant \alpha/48$, v^* takes values between $\alpha/2$ and $25\alpha/48$.

Implications for the full model. We now consider the extent to which our conclusions for the caricature system (2) can be extended to the full model (1). We address mathematical aspects only; their biological implications are discussed in Section 6.

In the caricature system, we have shown that there is a unique wave solution for u, for a given wave speed, and that this solution in turn determines a unique wave solution $V(z)$ for which $V = 0$ ahead of the wave. From this solution, we can read off $V(-\infty)$, which is the unique value of v^*. Thus, the decoupling of Equations (2a) and (2b) is crucial; recall that this property was chosen deliberately to mimic the decoupling of Equation (1a–f) from (1g–p) in the full model. Our numerical simulations suggest that in a manner analogous to the Fisher equation (2a), there is exactly one traveling wave solution of Equation (1a–f) for each speed above a critical minimum value. There are no theoretical results to back up this numerical observation, but if it is correct, the unique wave solution of Equation (1a–f) can be substituted into the traveling wave ordinary differential equations corresponding to Equation (1g–p), giving equations whose solution is uniquely determined by conditions ahead of the wave. These solutions in turn specify the healed collagen levels c_1^* and c_3^*.

Thus, the caricature model is highly analogous to the full model. This analogy suggests that the levels of collagen behind healing fronts in the full model will depend on the wave speed. We have confirmed this via numerical solutions in which the initial conditions decay exponentially to wounded

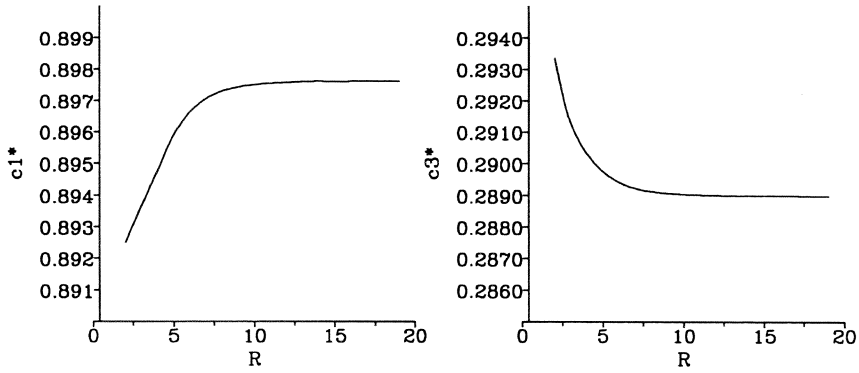

Figure 7. The change in the healed levels of collagen I and III when exponentially decaying initial conditions are imposed for model Equation (1). We note that the total variation in the healed levels due to a change in wave speed is about 1%.

states within the wound domain, rather than arising via a sudden transition. These initial conditions have no biological significance, and we use them simply to gain mathematical insight. As in the Fisher equation, sufficiently low initial decay rates do generate faster wavefronts, and these faster waves do indeed leave behind different collagen levels (Fig. 7). Again, our simulations suggest that these levels are uniquely determined by the wave speed, and that the total variation is very small (about 1%).

6. Discussion. Scar tissue formation following trauma or surgery is a major clinical problem, often resulting in poor wound strength or functional impairment. Adult wound healing entails a complex series of events involving many cell types and chemicals, and ultimately ending in scar formation. In contrast, fetal wounds heal more rapidly, with complete regeneration of the tissue and little or no scar. The ultimate aim of fetal wound-healing studies is thus to learn how to manipulate adult wounds so that they heal in a scarless, fetal-like fashion. Scar tissue is defined in terms of the density, diameter, and orientation of the collagen fibers within the wound domain. In adult wounds, thinner, more densely packed collagen fibers are observed, with the fibers being oriented along the lines of tension, in contrast to the basket-weave orientation of normal tissue. The diameter of the collagen fibers is related to the ratio of types I to III, with higher levels of type III collagen resulting in thinner fibers. Here, we present a model which aims to explain the difference between adult and fetal repair, by focusing on the final collagen levels and in particular on the ratio of collagen I to III. The model does not take into account the cell phenotype changes that may occur during dermal wound healing, known as dynamic reciprocity (Varedi *et al.*, 1995), which are the focus of other modeling studies (Olsen *et al.*, 1996, 1997).

We have developed a mathematical model which takes account of two different collagens and collagenases and two isoforms of TGFβ, as well as considering latent and active forms. We have used our model to investigate the effect of addition of isoform 1 or 3 of TGFβ during wound healing. Numerical simulations of the purely temporal model indicate that addition of TGFβ3 results in thicker collagen fibers, which is a characteristic of reduced scarring.

Experiments show clearly that such transient applications of TGFβs do cause permanent changes in collagen densities. However, this key feature is lost when we extend our model to reflect the influx of fibroblasts and growth factors from the surrounding unwounded dermis. In this spatiotemporal model, unique levels of collagen are selected behind healing wavefronts. To understand this mathematically, we have introduced a caricature model. This simple model also exhibits the behavior of a continuum of steady states, with only one particular state being selected behind wavefronts. Using this caricature model, we have shown that this steady-state selection occurs because there is a unique healing wavefront solution for the fibroblasts and growth factors, which in turn determines unique wave solutions for collagens and collagenases. The model was extended to take into account the chemotactic effect of TGFβ on the fibroblasts, but we found no significant change in behavior (results omitted for brevity). We thus neglected chemotaxis in the full spatial model.

An important issue is whether we can expect the differences between the temporal and spatiotemporal models to reflect real biological phenomena. We argue that we do expect this, based on our explanation for steady-state selection. As the fibroblasts migrate into the wound, the collagen and collagenase which are secreted have negligible interaction with the cells. Therefore, the decoupling of fibroblast and growth factor dynamics from those of collagens and collagenases means that any changes in the healed levels of collagen will reflect changes in fibroblast and growth factor evolution. In the purely temporal model, there is no stable healing solution, so that transient application of TGFβs causes a permanent change in the way in which fibroblast and growth factor levels evolve in subsequent healing. This results in new healed levels of collagens. By contrast, in the spatiotemporal model, the healing wavefront solution for fibroblasts and growth factors is stable, so that it rapidly recovers its form following transient applications of TGFβs. This in turn causes collagen levels to return to their pretreatment levels.

Thus, the underlying basis for the results of our spatiotemporal model is the existence of a stable healing wavefront of cells. Such stable fronts are a biological reality in other types of wound healing such as epithelial repair, in which cells are known to migrate in from the wound edges (Crosson *et al.*, 1986; Dale *et al.*, 1994). Thus, we can expect this phenomenon also to arise here if fibroblasts are entering the wound predominantly from the

surrounding dermis. Such an influx of cells would therefore imply that transient applications of TGFβs do not have a permanent effect on healed collagen levels, in contradiction to experimental observations. Hence, the migration of fibroblasts from the surrounding dermis alone cannot account for the permanent changes to collagen concentrations observed experimentally, and we conclude that migration of fibroblasts from the subcutaneous tissue plays a significant role in this process.

PDD acknowledges the Wellcome Trust for a Prize Studentship in Mathematical Biology. PKM thanks the Department of Mathematics, Williams College, Massachusetts, for their support and hospitality. Part of this work was done during a visit by PDD to the Department of Mathematics and Statistics, University of Canterbury, Christchurch, New Zealand. This work was supported in part by a grant from the London Mathematical Society. JAS and PKM were supported in part by Grant GR/K71394 from the EPSRC. The authors thank Professor M. W. J. Ferguson and Dr. M. Shah (University of Manchester) and Dr. J. C. Dallon (University of Warwick) for helpful discussions.

REFERENCES

Adzick, N. S. and M. T. Longaker. 1992. Characteristics of fetal tissue repair. In *Fetal Wound Healing*, N. S. Adzick and M. T. Longaker (Eds). New York: Elsevier, pp. 53–70.

Appling, W. D., W. R. O'Brien, D. A. Johnston and M. Duvie. 1989. Synergistic enhancement of type I and III collagen production in cultured fibroblasts by transforming growth factor-β and ascorbate. *FEBS Lett.* **250**, 541–544.

Armstrong, J. R. and M. W. J. Ferguson. 1995. Ontogeny of the skin and the transition from scar-free to scarring phenotype during wound healing in the pouch young of a marsupial, *Monodelphis domestica*. *Dev. Biol.* **169**, 242–260.

Bard, J. B. L. and E. D. Hay. 1975. The behaviour of fibroblasts from the developing avian cornea: morphology and movement *in situ* and *in vitro*. *J. Cell Biol.* **67**, 400–418.

Canosa, J. 1973. On a nonlinear diffusion equations describing population growth. *IBM J. Res. Dev.* **17**, 307–313.

Chaplain, M. A. J., S. M. Giles, B. D. Sleeman and R. J. Jarvis. 1995. A mathematical analysis of a model for tumour angiogenesis. *J. Math. Biol.* **33**, 744–770.

Chen, R. H., R. Ebner and R. Derynck. 1993. Inactivation of the type II receptor reveals two receptor pathways for the diverse TGFβ activities. *Science* **260**, 1335–1338.

Crosson, C. E., R. W. Klyce and R. W. Beuerman. 1986. Epithelial wound closure in the rabbit cornea. *Invest. Ophthal. Vis. Sci.* **27**, 464–473.

Dale, P. D., P. K. Maini and J. A. Sherratt. 1994. Mathematical modelling of corneal epithelial wound healing. *Math. Biosci.* **124**, 127–147.

Dale, P. D., J. A. Sherratt and P. K. Maini. 1996. A mathematical model for collagen fibre formation during foetal and adult dermal wound healing. *Proc. R. Soc. Lond. B* **263**, 653–660.

Ferguson, M. W. J. and G. F. Howarth. 1992. Marsupial models of scarless fetal wound healing. In *Fetal Wound Healing*, N. S. Adzick and M. T. Longaker (Eds). New York: Elsevier, pp. 95–124.

Fisher, R. A. 1937. The wave of advance of advantageous genes. *Ann. Eugen.* **7**, 353–369.

Flint, M. H., A. S. Craig, H. C. Reilly, G. C. Gillard and D. A. D. Parry. 1984. Collagen fibril diameters and glycosaminoglycan content of skins—indices of tissue maturity and function. *Connect. Tissue Res.* **13**, 69–81.

Jeffrey, J. J. 1992. Collagen degradation. In *Wound Healing: Biochemical and Clinical Aspects*, I. K. Cohen, R. F. Diegelmann and W. J. Lindblad (Eds). Philadelphia: W. B. Saunders, pp. 177–194.

Knight, K. R., D. A. Lepore, R. S. C. Horne, M. Ritz, J. V. Hurley, S. Kumta and B. M. O'Brien. 1993. Collagen content of uninjured skin and scar tissue in fetal and adult sheep. *Int. J. Exp. Pathol.* **74**, 583–591.

Kolmogoroff, A., I. Petrovsky and N. Piscounoff. 1937. Etude de l'équation de la diffusion avec croissance de la quantité de matière et son application à un problème biologique. *Moscow Univ. Bull. Math.* **1**, 1–25.

Krieg, T. 1995. Collagen in the healing wound. *Wounds* **7**, A5–A12.

Krummel, T. M., B. A. Michna, B. L. Thomas, M. B. Sporn, J. M. Nelson, A. M. Salzberg, I. K. Cohen and R. F. Diegelmann. 1988. Transforming growth factor beta induces fibrosis in a fetal wound model. *J. Pediatr. Surg.* **23**, 647–652.

Lin, R. Y., K. M. Sullivan, P. A. Argenta, M. Meuli, H. P. Lorenz and N. S. Adzick. 1995. Exogenous transforming growth factor beta amplifies its own expression and induces scar formation in a model of human fetal skin repair. *Annal Surg.* **222**, 146–154.

Martin, P., J. Hopkinson-Woolley and J. McCluskey. 1992. Growth factors and cutaneous wound repair. *Progr. Growth Factor Res.* **4**, 25–44.

Mast, B. A., J. M. Nelson and T. M. Krummel. 1992. Tissue repair in the mammalian fetus. In *Wound Healing: Biochemical and Clinical Aspects*, I. K. Cohen, R. F. Diegelmann and W. J. Lindblad (Eds). Philadelphia: W. B. Saunders, pp. 326–343.

McDonald, J. A. 1988. Fibronectin: a primitive matrix. In *The Molecular and Cellular Biology of Wound Repair*, R. A. F. Clark and P. M. Henson (Eds). New York: Plenum, pp. 405–436.

Merkel, J. R., B. R. DiPaolo, G. C. Hallcock and D. C. Rice. 1988. Type I and type III collagen content of healing wounds in fetal and adult rates. *Proc. Soc. Exp. Biol. Med.* **187**, 493–497.

Morgan, C. J. and W. J. Pledger. 1992. Fibroblast proliferation. In *Wound Healing: Biochemical and Clinical Aspects*, I. K. Cohen, R. F. Diegelmann and W. J. Lindblad (Eds). Philadelphia: W. B. Saunders, pp. 63–76.

Murphy, P. G., B. J. Loitz, C. B. Frank and D. A. Hart. 1994. Influence of exogenous growth factors on the synthesis and secretion of collagen type-I and type-III by explants of normal and healing rabbit ligaments. *Biochem. Cell Biol.* **72**, 403–409.

Murray, J. D., R. T. Tranquillo and P. K. Maini. 1988. Mechanochemical models for generating biological pattern and form in development. *Phys. Rep.* **171**, 59–84.

Olsen, L., J. A. Sherratt and P. K. Maini. 1996. A mathematical model for fibro-proliferative wound healing disorders. *Bull. Math. Biol.* **58**, 787–808.

Olsen, L., P. K. Maini, J. A. Sherratt and B. Marchant. (in press). Simple modelling of extracellular matrix alignment in dermal wound healing. I. Cell flux induced alignment.

Peacock, E. E. 1984. *Wound Repair*. Philadelphia: W. B. Saunders.

Pierce, G. F., D. Brown and T. A. Mustoe. 1991. Quantitative analysis of the inflammatory cell influx, procollagen type I synthesis, and collagen cross-linking in incisional wounds: influence of PDGF-BB and TGF-β1 therapy. *J. Lab. Clin. Med.* **117**, 373–382.

Roberts, A. B. and M. B. Sporn. 1990. The transforming growth factor-βs. In *Peptide Growth Factors and Their Receptors*, M. B. Sporn and A. B. Roberts (Eds). Berlin: Springer-Verlag, pp. 419–472.

Rothe, F. 1978. Convergence to travelling fronts in semilinear parabolic equations. *Proc. R. Soc. Edin.* **80A**, 213–234.

Shah, M., D. M. Foreman and M. W. J. Ferguson. 1992. Control of scarring in adult wounds by neutralising antibody to transforming growth factor β. *Lancet* **339**, 213–214.

Shah, M., D. M. Foreman and M. W. J. Ferguson. 1994. Neutralizing antibody to TGFβ(1,2) reduces scarring in adult rodents. *J. Cell Sci.* **107**, 1137–1157.

Shah, M., D. M. Foreman and M. W. J. Ferguson. 1995. Neutralization of TGFβ1 and TGFβ2 or exogenous addition of TGFβ3 to cutaneous rat wounds scarring. *J. Cell Sci.* **108**, 985–1002.

Sherratt, J. A. and J. D. Murray. 1990. Models of epidermal wound healing. *Proc. R. Soc. Lond. B* **241**, 29–36.

Sinclair, R. D. and T. J. Ryan. 1994. Proteolytic enzymes in wound healing: the role of enzymatic debridement. *Austr. J. Dermatol.* **35**, 35–41.

Streuli, C. H., C. Schmidhauser, M. Kobrin, M. J. Bissell and R. Derynck. 1993. Extracellular matrix regulates expression of the TGF-β1 gene. *J. Cell Biol.* **120**, 253–260.

Stricklin, G. P., E. A. Bauer and J. J. Jeffrey. 1978. Human skin collagenase: chemical properties of precursor and active forms. *Biochemistry* **17**, 2331–2337.

Varedi, M., E. E. Tredget, P. G. Scott, Y. J. Shen and A. Ghahary. 1995. Alteration in cell morphology triggers transforming growth factor beta 1, collagenase, and tissue inhibitor of metalloproteinases I expression in normal and hypertrophic scar fibroblasts. *J. Invest. Dermatol.* **104**, 118–123.

Whitby, D. J. and M. W. J. Ferguson. 1991. Immunohistochemical localization of growth factors in fetal wound healing. *Dev. Biol.* **147**, 207–215.

Whitby, D. J. and M. W. J. Ferguson. 1992. Immunohistochemical studies of the extracellular matrix and soluble growth factors in fetal and adult wound healing. In *Fetal Wound Healing*, N. S. Adzick and M. T. Longaker (Eds). New York: Elsevier, pp. 161–176.

Zhang, K., W. Garner, L. Cohen, J. Rodriguez and S. Phan. 1995. Increased type I and type III collagen and transforming growth factor β-1 messenger RNA and protein in hypertrophic burn scar. *J. Invest. Dermatol.* **104**, 750–754.

Received 2 May 1996
Revised version accepted 5 May 1997